

# Comparative Morphological Analysis of the Geometry of Ruptured and Unruptured Aneurysms

Aichi Chien, PhD\*

James Sayre, PhD‡

Fernando Viñuela, MD\*

\*Division of Interventional Neuroradiology, David Geffen School of Medicine, and ‡Department of Biostatistics, School of Public Health, University of California, Los Angeles, California

**Correspondence:**

Aichi Chien, PhD,  
Division of Interventional  
Neuroradiology,  
David Geffen School of Medicine at  
UCLA, 10833 LeConte Ave, Box 951721,  
Los Angeles, CA 90095.  
E-mail: aichi@ucla.edu

**Received,** April 20, 2010.

**Accepted,** January 28, 2011.

**Published Online,** March 15, 2011.

Copyright © 2011 by the  
Congress of Neurological Surgeons

**BACKGROUND:** The risk of aneurysm rupture appears to be related to multiple factors such as topology, morphology, size, perianeurysmal environment, and blood flow hemodynamics.

**OBJECTIVE:** To evaluate aneurysm morphology and to quantitatively compare the volumetric parameters between ruptured and unruptured aneurysms from our clinical database at the UCLA Medical Center.

**METHODS:** Novel algorithms that automatically compute aneurysm geometry were tested on the basis of voxel data obtained from angiographic images, and measurements of aneurysm morphology were automatically recorded. We studied a total of 50 aneurysms (25 ruptured and 25 unruptured) with sizes ranging from 3 to 26 mm. To compare the geometric characteristics between ruptured and unruptured groups, we examined measurements, including volume and surface area, and the ratios of these measurements to the minimal bounding sphere around each aneurysm.

**RESULTS:** More than 65% of ruptured aneurysms had a ratio of aneurysm volume to bounding sphere volume (AVSV) of  $> 0.5$ . More than 70% of ruptured aneurysms had a ratio of aneurysm surface to bounding sphere surface (AASA) of  $< 1$ . A trend differentiating ruptured and unruptured aneurysms was observed in AVSV ( $P = .07$ ) and AASA ( $P = .04$ ). Classification and regression trees analysis showed 68% correct classification with rupture for AVSV and 70% for AASA.

**CONCLUSION:** By comparing aneurysm geometry with the bounding sphere, we found a trend associating the ratios of aneurysm volume and surface area with rupture. These geometric parameters may be useful for understanding the influence of morphology on the risk of aneurysm rupture.

**KEY WORDS:** Aneurysm rupture, Geometry, Quantitative, Surface area, Volume

*Neurosurgery* 69:349–356, 2011

DOI: 10.1227/NEU.0b013e31821661c3

www.neurosurgery-online.com

The risk of aneurysm rupture appears to be related to aneurysm site, size, morphology, blood flow hemodynamics, perianeurysmal environment, and patient history, among other factors.<sup>1–5</sup> By measuring the width and angle of aneurysms from images, yielding characteristics such as the aspect ratio (depth/neck width), studies have suggested that

geometric measurements may be useful for predicting aneurysm rupture.<sup>6–8</sup> Furthermore, quantifying aneurysm shape can be an effective approach to discriminate ruptured and unruptured aneurysms, as shown with Fourier analysis and shape indexes.<sup>9–11</sup> Still, although many large studies have defined critical size by the aneurysm maximal dimension, research investigating the association of aneurysm geometric characteristics with rupture is limited.

In this study, we analyzed aneurysm geometry from our clinical database and studied the morphological difference between ruptured and unruptured aneurysms. An algorithm developed in-house was used in 50 aneurysms to compute their volume and shape automatically.<sup>12</sup> Because

**ABBREVIATIONS:** AASA, ratio of aneurysm surface to bounding sphere surface; AVSV, ratio of aneurysm volume to bounding sphere volume; CTA, computed tomography angiography; FDA, Food and Drug Administration; HGC, high gaussian curvature; HMC, high mean curvature; RA, rotational angiography

aneurysm blebs, shown as a sudden increase in local curvature, are important features to be characterized, we also compared the 3-dimensional (3D) curvatures of aneurysms in the volumetric analysis. Parameters that we examined included volume, surface area, and high curvature areas for each aneurysm. Our aim was to quantitatively evaluate 3D morphology and to efficiently compare geometric parameters of ruptured and unruptured aneurysms.

## MATERIALS AND METHODS

### Case Selection

Brain aneurysms located at internal carotid artery, middle cerebral artery, anterior communicating artery, posterior communicating artery, and basilar artery locations were selected from an aneurysm database that recorded aneurysms treated consecutively from January 2006 to July 2008 in the Division of Interventional Neuroradiology, UCLA Medical Center. Only aneurysms that had pre-embolization angiograms acquired by either 3D rotational angiography (RA) or 3D computed tomography angiography (CTA) were considered in this study. For each location, 5 ruptured aneurysms and 5 unruptured aneurysms were selected in chronological order. A total of 50 aneurysms (25 ruptured and 25 unruptured) were included. Patients' ages ranged from 29 to 82 years; there were 10 men and 36 women. Aneurysm size (largest dimensions in the aneurysm dome) was  $9.1 \pm 5.1$  mm on average with a range from 3 to 25.6 mm. Table 1 summarizes the details of the cases.

### Geometric Analyses

Three-dimensional angiographic images were used to reconstruct aneurysm geometry. Fifteen aneurysms (6 ruptured and 9 unruptured) were acquired by CTA (Sensation 16, Siemens, Munich, Germany). Thirty-five aneurysms (19 ruptured and 16 unruptured) were obtained by RA (Integris unit, Philips, Best, the Netherlands), and their volume data was used to reconstruct the aneurysm geometry. Images were transferred to a desktop computer (Dell OptiPlex G×620) for volumetric analysis. Software developed in-house that was based on level set methods and fast sweeping methods was used for the automatic volumetric analysis and 3D reconstruction for each aneurysm with MATLAB (The Mathworks Inc, Natick, Massachusetts) (Figure 1A).<sup>12-14</sup>

Because aneurysm size is commonly specified by the maximum width that approximates an aneurysm by its bounding sphere, we studied the geometric properties with respect to their deviation from the spherical shape. The ratios of 3 basic geometric parameters—volume, surface area, and curvature—were analyzed. Each aneurysm was automatically segmented after denoting the aneurysm location (Figure 1B). A minimal bounding sphere was defined around each aneurysm using the 2 most distant points on the surface (Figure 1C). Aneurysm volume, the ratio of the aneurysm volume to sphere volume (AVSV), aneurysm surface area, and the ratio of the aneurysm surface area to sphere surface area (AASA) were automatically collected.

To capture the morphological characteristics of aneurysm blebs, which are usually shown as sudden increases in local curvature, curvatures of ruptured and unruptured aneurysms were also compared. The curvature of any point on a curve can be found by the circle approximating the curve at that point; for example, the curvature at any point on a circle with radius  $r$  is constant and equal to  $1/r$ . Curvatures on a surface are more complicated because for any given point there are many possible

**TABLE 1. Summary of Aneurysm Cases**

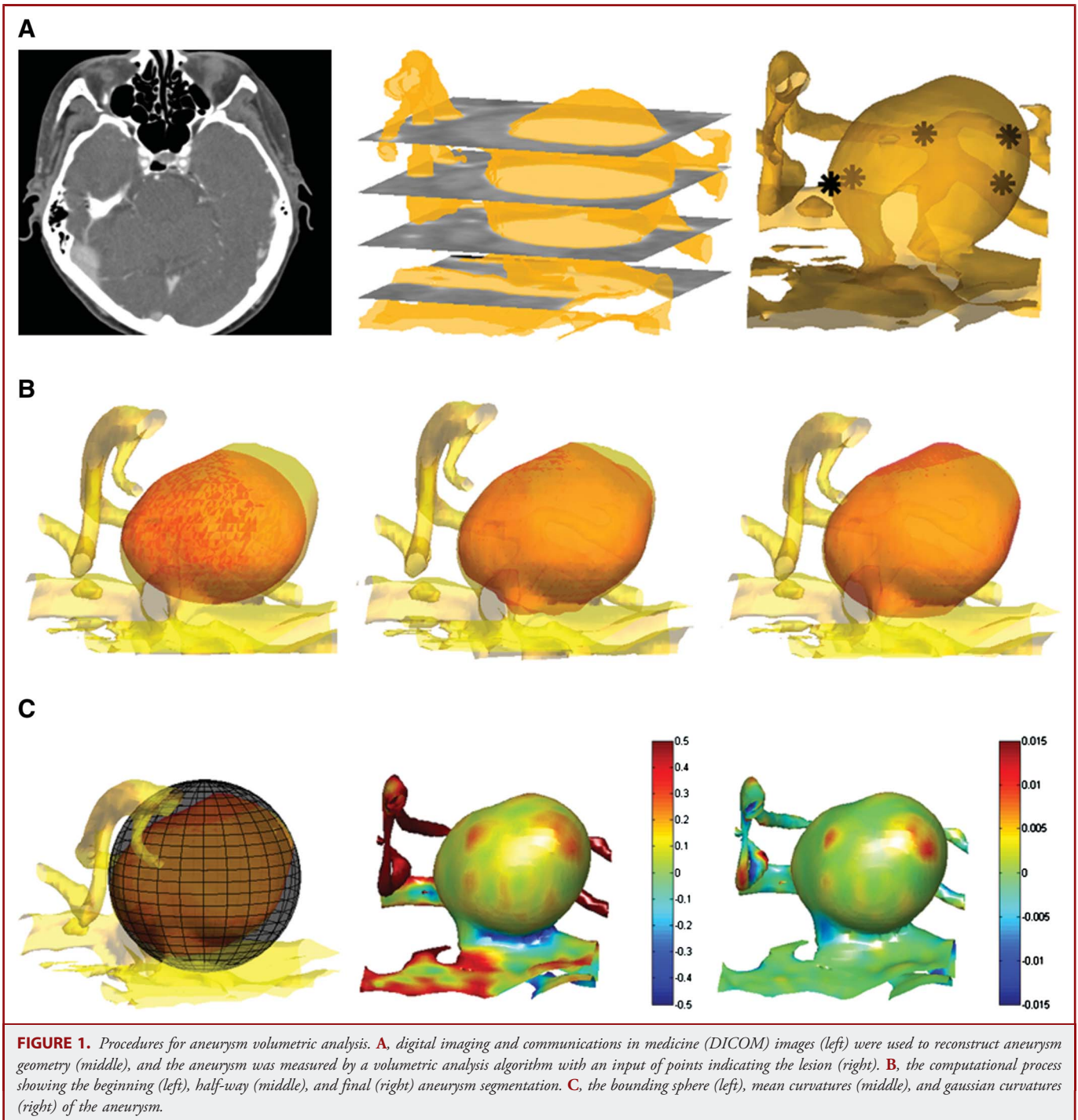
Characteristics	Ruptured Aneurysm (n = 25)	Unruptured Aneurysm (n = 25)	Summary
<b>Age, y</b>			
Mean	61.8	58.5	60.2
Range	38-82	29-82	29-82
<b>Sex, n</b>			
Female	16	20	36
Male	8	2	10
<b>Location of aneurysm, n</b>			
Internal carotid artery	5	5	10
Middle cerebral artery	5	5	10
Anterior communicating artery	5	5	10
Posterior communicating artery	5	5	10
Basilar artery	5	5	10
Aneurysms with blebs, n	10	8	18
<b>Largest diameter of aneurysm, mm</b>			
Mean	9.7	8.6	9.1
Range	3.0-25.6	4.0-18.6	3.0-25.6
<b>Diameter of aneurysm neck, mm</b>			
Mean	4.2	4.3	4.25
Range	2.0-9.0	2.2-9.8	2.0-9.8
<b>Size of aneurysm, n</b>			
< 7 mm	12	11	23
7-12 mm	8	10	18
13-26 mm	5	4	9

curves that can lie on that point; therefore, various methods can be used to describe the curvature.<sup>15</sup>

Recently, curvatures, in particular mean curvature and gaussian curvature, have been proposed in several studies to analyze aneurysm shapes.<sup>9,16,17</sup> (The mean curvature is the average of the principal curvatures, and gaussian curvature is the product of principal curvatures.<sup>15</sup>) In our analysis, we also computed these 2 curvature measurements. Because aneurysm blebs tend to have higher curvature, we used the curvature of the bounding sphere as the baseline and found the high mean curvature (HMC), the mean curvature higher than the mean curvature of the bounding sphere, and high gaussian curvature (HGC), the gaussian curvature higher than the gaussian curvature of bounding sphere, to investigate the curvature difference between ruptured and unruptured aneurysms. Examples of changes in geometric properties of a simple round aneurysm and an aneurysm with bleb are illustrated in Figure 2.

### Technique Validation

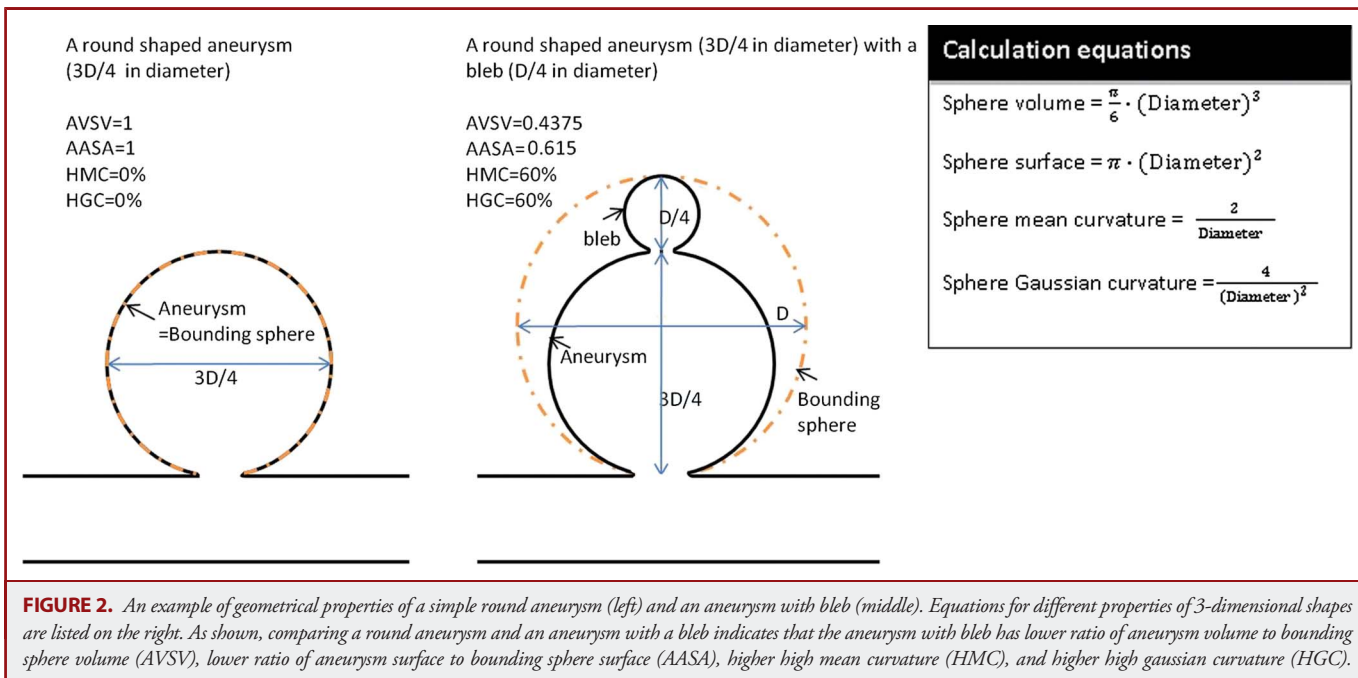
We validated the automatic volumetric analysis by comparing with phantom data provided by the US Food and Drug Administration (FDA).<sup>18</sup> Phantoms were made in spherical shapes with diameters of 5, 8, and 10 mm, size ranges similar to brain aneurysms. Three-dimensional CT imaging was used to acquire geometric data. Two phantoms for each size were analyzed. Five measurements were made for each phantom to test the repeatability of automatic analysis and compared with the reported measurements.



**Statistical Analysis**

Results are expressed as mean and standard deviation. Nonparametric analyses, Kolmogorov-Smirnov tests, were used to compare parameter distributions between ruptured and unruptured cases, and Spearman  $\rho$  analyses were used to find correlations between parameters. Classification and regression trees analyses were applied to find the correct classification

of rupture within each parameter. We used  $t$  tests to examine the accuracy of the volumetric analysis in the validation study. The statistical significance level was set at 0.05. SPSS (PASW) version 17.0 (SPSS Inc, Chicago, Illinois) and classification and regression trees software version 6.0 (Salford System, San Diego, California) were used to perform statistical analyses.



## RESULTS

Average aneurysm volumes were  $424.8 \pm 911.6 \text{ mm}^3$  in all aneurysms,  $631.7 \pm 1242.1 \text{ mm}^3$  in ruptured aneurysms, and  $218.0 \pm 254.2 \text{ mm}^3$  in unruptured aneurysms. Average aneurysm surface areas were  $651.6 \pm 1457.8 \text{ mm}^2$  in all aneurysms,  $793.5 \pm 1927.0 \text{ mm}^2$  in ruptured aneurysms, and  $509.7 \pm 764.0 \text{ mm}^2$  in unruptured aneurysms. No statistical difference was found between groups in measurements of volume and surface area. Figure 3 shows a representative aneurysm volumetric analysis. The 3D reconstruction of a basilar trunk aneurysm (18.7-mm diameter) is shown in Figure 3. The automatic computation was initiated by giving a few points to locate the aneurysm. The geometric analysis successfully calculated the boundary of the aneurysm, as shown in Figure 3D.

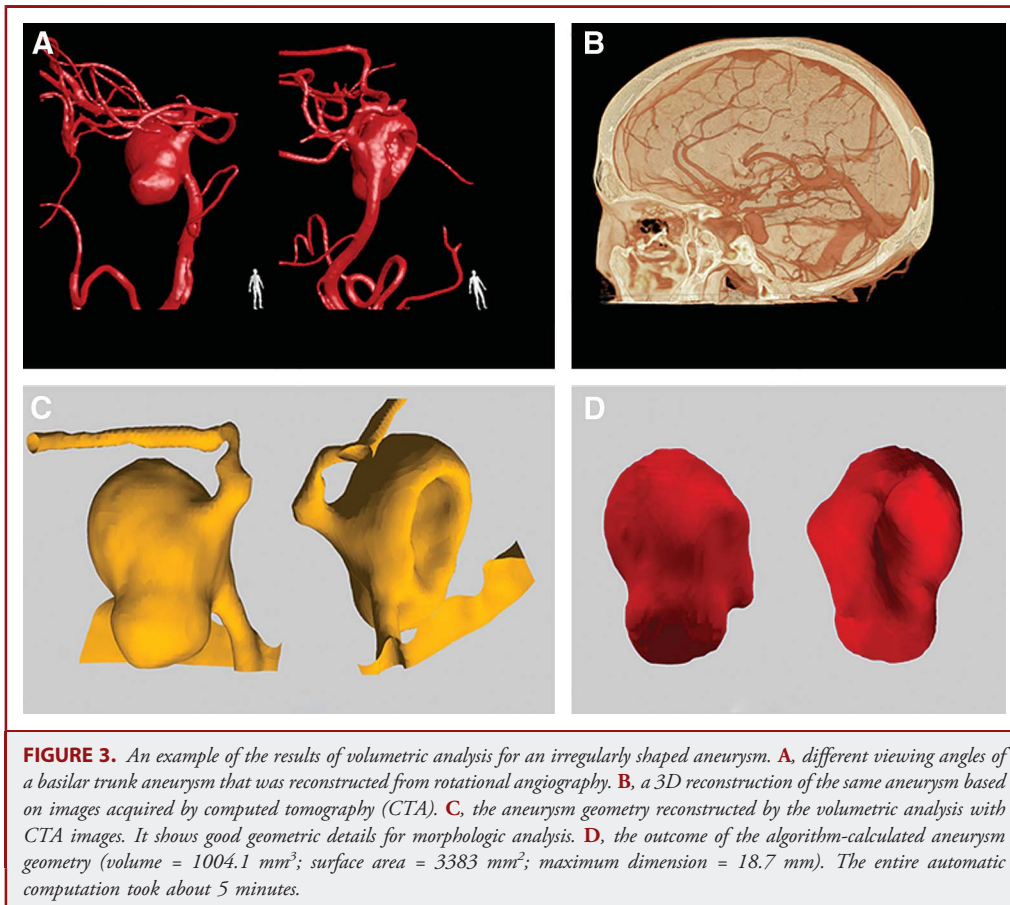
The average AVSV was  $0.48 \pm 0.12$  in all aneurysms,  $0.49 \pm 0.11$  in ruptured aneurysms, and  $0.47 \pm 0.12$  in unruptured aneurysms. However,  $> 65\%$  of ruptured aneurysms had an AVSV  $> 0.5$ , whereas about 30% of unruptured aneurysms had an AVSV  $> 0.5$ . A trend of difference ( $P = 0.07$ ) was found in AVSVs between the ruptured and unruptured groups. Classification and regression trees analysis showed 68% correct classification with rupture at an AVSV  $\geq 0.5$ . The average AASA was  $1.2 \pm 0.8$  in all aneurysms,  $1.1 \pm 0.9$  in ruptured aneurysms, and  $1.3 \pm 0.7$  in unruptured aneurysms. More than 70% of ruptured aneurysms had an AASA  $< 1$ , whereas about 40% of unruptured aneurysms had an AASA  $< 1$  and 44% had an AASA in the range of 1.0 to 1.9. The AASA was found to be able to differentiate ruptured and unruptured groups with statistical

significance ( $P = .04$ ) and 70% correct classification with rupture at an AASA  $\leq 0.86$ . The average HMC was  $7.1 \pm 7.0\%$  in all aneurysms,  $5.9 \pm 6.8\%$  in ruptured aneurysms, and  $8.2 \pm 7.4\%$  in unruptured aneurysms. The average HGC was  $29.1 \pm 9.2\%$  in all aneurysms,  $28.9 \pm 10.0\%$  in ruptured aneurysms, and  $29.3 \pm 8.6\%$  in unruptured aneurysms. We did not find statistical differences between the ruptured and unruptured groups in either HMC or HGC. Among 6 parameters, only AVSV was minimally correlated to aneurysm size ( $\rho = 0.074$ ,  $P = .61$ ); other parameters showed significant correlation to aneurysm size ( $P < .01$ ). Results are shown in Table 2 and Figure 4.

The automatic volumetric analysis of the FDA phantom showed good agreement with the reported phantom measurements.<sup>18</sup> Five independent volume calculations for 5-, 8-, and 10-mm phantoms were  $58.0 \pm 2.6$ ,  $505.2 \pm 5.2$ , and  $265.4 \pm 6.5 \text{ mm}^3$ . No statistical differences were found compared with the FDA-reported data or between repeated automatic measurements.

## DISCUSSION

Although aneurysm morphology may be an important factor related to rupture, detailed study of the relationship is limited. Researchers have suggested that shape parameters are more effective measurements to evaluate aneurysm risk of rupture than aneurysm size.<sup>7,9</sup> Currently, however, reports of morphological analysis have focused mainly on aneurysms around 6 mm in size.<sup>7,9</sup> The present study examined aneurysms ranging in size from 3 to 25 mm and compared geometric parameters between ruptured and unruptured



cases. Through computing volume, surface area, curvature, and their ratios to the bounding sphere, we analyzed 6 geometric parameters. We found that AVSV and AASA showed a trend differentiating between ruptured and unruptured aneurysms.

The AVSV and AASA are similar to shape indexes to capture the irregular features of aneurysm.<sup>9</sup> The AVSV is the ratio of aneurysm volume with respect to its bounding sphere. When an aneurysm shape is a sphere, AVSV is equal to 1. Because none of the aneurysms has a perfectly spherical shape, we observed AVSV to always be  $< 1$ . We found that the majority of the ruptured aneurysms have an AVSV in the range of 0.50 to 0.59. This may suggest an important volume ratio to assess risk of aneurysm rupture. The AASA is the ratio of aneurysm surface area with respect to its bounding sphere and represents the irregularity of the surface area. An AASA of 1 would mean that the aneurysm is a perfect sphere. The AASA is statistically different between the ruptured and unruptured groups, with  $> 70\%$  of the ruptured aneurysms having an AASA of  $< 1$ . The AASA may also be a good morphological parameter to characterize morphology quantitatively and to assess rupture risk. Although changes in curvature can be observed at aneurysm blebs, we did not find statistical differences between ruptured

and unruptured groups when comparing HMC and HGC, the curvature parameters. The reason may be that quantification of curvatures is also influenced by other shape features as indicated by a previous study.<sup>9</sup>

Raghavan et al<sup>9</sup> suggested that evaluating aneurysm shape on the basis of the ratio of volume and surface area is more effective than using aneurysm volume and surface area to discriminate between ruptured and unruptured aneurysms. In our study, aneurysm volume and surface area also did not show statistical difference between rupture and unruptured groups. Because these 2 parameters are also correlated to the size of aneurysms (volume  $\rho = 0.976$ ,  $P < .001$ ; surface area  $\rho = 0.95$ ,  $P < .001$ ), the null results may be influenced by the case enrollment. Further study with combined cases from other institutes is needed to determine whether measurements of aneurysm volume and surface are associated with rupture. Moreover, surface area reflects the irregularity of the aneurysm wall. Although in general surface area increases with an increase in maximum dimension, a broad range of variation was found in both the ruptured and unruptured groups. Research into surface variation with a fixed size range is needed to fully understand the risk of rupture with this geometric quantity.

**TABLE 2. Ratio of Aneurysm Geometry to the Bounding Sphere for Ruptured and Unruptured Aneurysms**

	Ruptured Aneurysms, n (%)	Unruptured Aneurysms, n (%)
<b>AVSV</b>		
< 0.3	3 (12)	2 (8)
0.3–0.39	2 (8)	5 (20)
0.4–0.49	3 (12)	10 (40)
0.5–0.59	13 (52)	3 (12)
≥ 0.6	4 (16)	5 (20)
<b>AASA</b>		
< 1.0	18 (72)	10 (40)
1.0–1.9	4 (16)	11 (44)
> 2.0	3 (12)	4 (16)
<b>HMC, %</b>		
< 5	3 (12)	2 (8)
5–10	11 (44)	11 (44)
> 10	11 (44)	12 (48)
<b>HGC, %</b>		
< 20	3 (12)	3 (12)
20–30	9 (36)	10 (40)
> 30	13 (52)	12 (48)

On the basis of the quantitative analysis, we found a trend of higher AVSV ( $AVSV \geq 0.5$ ) and lower AASA ( $AASA \leq 0.86$ ) in ruptured aneurysms. Our hypothesis is that these results may be related to the tissue mechanical properties of aneurysm wall. Using nonlinear finite-element analysis, studies have reported the importance of shape and how it influences the wall stress and stretch in the tissue.<sup>19,20</sup> Higher AVSV observed in ruptured aneurysms may be explained by the greater extent of stress and stretch in more spherical aneurysms, as shown by Kyriacou and Humphrey<sup>19</sup> when comparing the mechanical stress in aneurysms with the same volume but different shape. The AASA is related to the Green strain and inversely proportional to the stretch ratio.<sup>19,21</sup> This suggests that aneurysms with lower AASA may have larger stretch at the aneurysm wall and may explain the low AASA found in the majority of the ruptured aneurysms in our study. In the future, research with more cases and combining geometric analysis with tissue mechanics will be useful to better understand the meaning of AVSV and AASA. Moreover, incorporating other morphological properties of aneurysms such as the shape of the aneurysm neck into the analysis will be important to help relate the volumetric parameters to other shape indexes such as aspect ratio.<sup>22</sup>

The large difference in the average volume of ruptured and unruptured aneurysms is due to the size difference between groups. The largest aneurysms in the ruptured and unruptured group are 25.6 and 18.6 mm, respectively. Because volume is the cube of the linear dimension, a small increase in the largest

dimension results in dramatic increases in volume. For example, the volume of 3- and 4-mm spherical aneurysms is 14 and 33 mm<sup>3</sup>, respectively, and the difference between their volumes is 19 mm<sup>3</sup>. As shown in Table 1, aneurysms in the ruptured group were larger. This difference between groups is amplified when volume is considered.

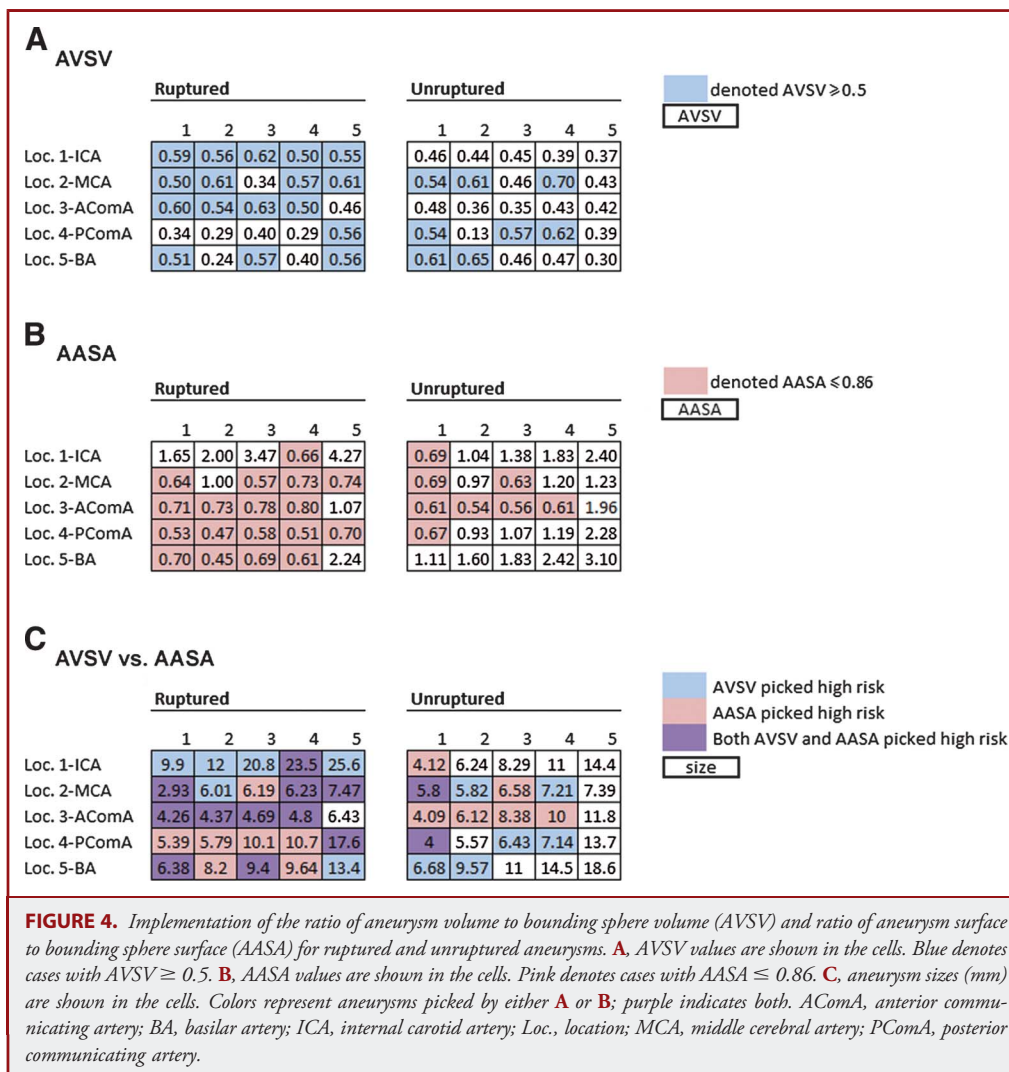
In this study, we used software developed in-house to compute aneurysm geometry and found that AVSV and AASA may be useful to assess risk of rupture regardless of aneurysm size. Figure 4 shows the implementation of these 2 parameters for the ruptured and unruptured groups. In addition, AVSV and AASA can be obtained by other software,<sup>7,9,23</sup> making them practical for implementation in large clinical studies in the future.

### Limitations

We studied ruptured aneurysms by analyzing the geometry based on angiographic images taken within 24 hours of a subarachnoid hemorrhage. It is unclear how aneurysms change as a result of rupture; both increases and decreases in size after rupture have been reported.<sup>24,25</sup> Some studies have also suggested that there are no major changes in aneurysm shape as a result of rupture.<sup>10,26,27</sup> Because of the difficulty of acquiring angiographic images of ruptured aneurysms before subarachnoid hemorrhage, research that compares the geometrical characteristics of ruptured and unruptured aneurysms has applied the assumption that aneurysm shape does not change owing to rupture.<sup>6,9,10,28</sup> In our analysis, we also assumed that aneurysm rupture does not influence the geometric configuration. Further study that analyzes aneurysm geometry before and after rupture is important to elucidate the shape and size changes resulting from the rupture and to re-examine this hypothesis. Collecting image data before and after aneurysm rupture and using the present morphology analysis technique to study aneurysm geometric changes caused by rupture will be our future tasks.

In this study, because of the variation of aneurysm sizes and shapes, ruptured and unruptured aneurysms were not matched according to their greatest dimension. Furthermore, the small number of cases and combinations of different aneurysmal sites was limiting. In the future, comparing morphology between ruptured and unruptured aneurysms in a larger clinical series with matched location and matched size, or an overall narrower range of sizes, is needed to provide more complete information on the morphological differences in ruptured and unruptured aneurysms.

To incorporate more cases into the study, patients who satisfied the selection criteria but did not have pre-embolization 3D RA images were included in the study if their 3D CTA image data were available. Although in the past we have found that CTA can provide high-quality information for aneurysm geometric measurements,<sup>29,30</sup> the differences in calculation error associated with the source imaging modality need to be analyzed. A study identifying aneurysms with both pre-embolization 3D RA and 3D CTA images is ongoing and is investigating how the geometric analysis is affected by different imaging modalities.



We focused on the geometric analysis of aneurysms in our clinical database in which the collection of cases may be biased as a result of the patient referral pattern in our center. Future study combining cases from different institutions is needed. As indicated by previous reports, morphology analysis, coupled with the geometry of the parent artery, may provide additional information to study aneurysm rupture.<sup>7,8</sup> Incorporating vascular geometry into the calculation is essential to improve the aneurysm volumetric analysis.

**CONCLUSION**

We used volumetric analysis to study the geometry of 50 aneurysms. Through quantitative comparison, a trend of difference between the ruptured and unruptured groups in AVSV and AASA was found. These 2 parameters may be useful for describing aneurysm morphology and for studies of aneurysm risk of rupture. The techniques we have applied translate well to large studies that could further confirm our observations.

**Disclosure**

This FDA collection was supported by the FDA Critical Path Initiative, National Cancer Institute, and National Institute of Biomedical Imaging and Bioengineering. The authors have no personal financial or institutional interests in any of the drugs, materials, or devices described in this article.

**REFERENCES**

1. Unruptured intracranial aneurysms: risk of rupture and risks of surgical intervention: International Study of Unruptured Intracranial Aneurysms Investigators. *N Engl J Med.* 1998;339(24):1725- 1733.
2. Wermer MJ, van der Schaaf IC, Algra A, Rinkel GJ. Risk of rupture of unruptured intracranial aneurysms in relation to patient and aneurysm characteristics: an updated meta-analysis. *Stroke.* 2007;38(4):1404-1410.
3. Wiebers DO, Whisnant JP, Huston J III, et al. Unruptured intracranial aneurysms: natural history, clinical outcome, and risks of surgical and endovascular treatment. *Lancet.* 2003;362(9378):103-110.
4. Chien A, Tatushima S, Sayre J, Castro M, Cebal J, Vinuela F. Patient-specific hemodynamic analysis of small internal carotid artery-ophthalmic artery aneurysms. *Surg Neurol.* 2009;72(5):444-450.

5. Chien A, Castro MA, Tateshima S, Sayre J, Cebral J, Vinuela F. Quantitative hemodynamic analysis of brain aneurysms at different locations. *AJNR Am J Neuroradiol*. 2009;30(8):1507-1512.
6. Ujjie H, Tamano Y, Sasaki K, Hori T. Is the aspect ratio a reliable index for predicting the rupture of a saccular aneurysm? *Neurosurgery*. 2001;48(3):495-502.
7. Dhar S, Tremmel M, Mocco J, et al. Morphology parameters for intracranial aneurysm rupture risk assessment. *Neurosurgery*. 2008;63(2):185-196.
8. Sadatomo T, Yuki K, Migita K, Taniguchi E, Kodama Y, Kurisu K. Morphological differences between ruptured and unruptured cases in middle cerebral artery aneurysms. *Neurosurgery*. 2008;62(3):602-609.
9. Raghavan ML, Ma B, Harbaugh RE. Quantified aneurysm shape and rupture risk. *J Neurosurg*. 2005;102(2):355-362.
10. Rohde S, Lahmann K, Beck J, et al. Fourier analysis of intracranial aneurysms: towards an objective and quantitative evaluation of the shape of aneurysms. *Neuroradiology*. 2005;47(2):121-126.
11. Hademenos GJ, Massoud TF, Turjman F, Sayre JW. Anatomical and morphological factors correlating with rupture of intracranial aneurysms in patients referred for endovascular treatment. *Neuroradiology*. 1998;40(11):755-760.
12. Dong B, Chien A, Mao Y, Ye J, Osher S. Level set based surface capturing in 3D medical images. *Med Image Comput Assist Interv*. 2008;11(pt 1):162-169.
13. Tsai R, Cheng L, Osher S, Zhao H. Fast sweeping algorithms for a class of Hamilton-Jacobi equations. *SIAM J Numerical Anal*. 2003;41(2):673-694.
14. Osher S, Fedkiw R. *Level Set Methods and Dynamic Implicit Surfaces*. Volume 153. New York, NY: Springer-Verlag; 2003.
15. Spivak M. *A Comprehensive Introduction to Differential Geometry*. 2nd ed. Berkeley, CA: Publish or Perish, Inc; 1979.
16. Hoi Y, Meng H, Woodward SH, et al. Effects of arterial geometry on aneurysm growth: three-dimensional computational fluid dynamics study. *J Neurosurg*. 2004;101(4):676-681.
17. Ma B, Harbaugh RE, Raghavan ML. Three-dimensional geometrical characterization of cerebral aneurysms. *Ann Biomed Eng*. 2004;32(2):264-273.
18. Kinnard L, Gavrielides M, Myers K, et al. Volume error analysis for lung nodules attached to pulmonary vessels in an anthropomorphic thoracic phantom. *SPIE Medical Imaging*. 2008;6915:69152Q-69159Q.
19. Kyriacou SK, Humphrey JD. Influence of size, shape and properties on the mechanics of axisymmetric saccular aneurysms. *J Biomech*. 1996;29(8):1015-1022.
20. Chien A, Shoucri RM, Mal A, Montemagno CD. Human cardiac wall stress analysis with patient-specific myocardial material properties. *Model Med Biol VII*. 2007;12:33-42.
21. Green AE, Adkins JE. *Large Elastic Deformations and Nonlinear Continuum Mechanics*. London, UK: Oxford University Press; 1960.
22. Ujjie H, Tachibana H, Hiramatsu O, et al. Effects of size and shape (aspect ratio) on the hemodynamics of saccular aneurysms: a possible index for surgical treatment of intracranial aneurysms. *Neurosurgery*. 1999;45(1):119-129.
23. Piotin M, Daghman B, Mounayer C, Spelle L, Moret J. Ellipsoid approximation versus 3D rotational angiography in the volumetric assessment of intracranial aneurysms. *AJNR Am J Neuroradiol*. 2006;27(4):839-842.
24. Wiebers DO, Whisnant JP, O'Fallon WM. The natural history of unruptured intracranial aneurysms. *N Engl J Med*. 1981;304(12):696-698.
25. Yasui N, Magarisawa S, Suzuki A, Nishimura H, Okudera T, Abe T. Subarachnoid hemorrhage caused by previously diagnosed, previously unruptured intracranial aneurysms: a retrospective analysis of 25 cases. *Neurosurgery*. 1996;39(6):1096-1100.
26. Kataoka K, Taneda M, Asai T, Kinoshita A, Ito M, Kuroda R. Structural fragility and inflammatory response of ruptured cerebral aneurysms: a comparative study between ruptured and unruptured cerebral aneurysms. *Stroke*. 1999;30(7):1396-1401.
27. Kataoka K, Taneda M, Asai T, Yamada Y. Difference in nature of ruptured and unruptured cerebral aneurysms. *Lancet*. 2000;355(9199):203.
28. Beck J, Rohde S, el Beltagy M, et al. Difference in configuration of ruptured and unruptured intracranial aneurysms determined by biplanar digital subtraction angiography. *Acta Neurochir (Wien)*. 2003;145(10):861-865.
29. Villablanca JP, Hooshi P, Martin N, et al. Three-dimensional helical computerized tomography angiography in the diagnosis, characterization, and management of middle cerebral artery aneurysms: comparison with conventional angiography and intraoperative findings. *J Neurosurg*. 2002;97(6):1322-1332.
30. Villablanca JP, Martin N, Jahan R, et al. Volume-rendered helical computerized tomography angiography in the detection and characterization of intracranial aneurysms. *J Neurosurg*. 2000;93(2):254-264.

## Acknowledgment

We gratefully acknowledge Nicholas Petrick, PhD, from the US Food and Drug Administration CDRH/OSEL/DIAM for providing phantom data. We are also grateful to Bin Dong and Jian Ye for assistance with programming.

## COMMENT

Chien and colleagues present a comparative analysis of morphological characteristics in ruptured and unruptured aneurysms. They use several novel morphological assessments, the most important of which is based on a calculated "minimal bounding sphere," in an attempt to capture mathematically the intricate variations in dimensions of intracranial aneurysms. As the authors correctly state, the use of greatest diameter either to assess risk of future rupture or to determine site of rupture in a patient with multiple intracranial aneurysms is antiquated. Unfortunately, greatest dimension remains the standard among the majority of neurosurgeons in practice. Increasing evidence indicates that other morphological characteristics and the relationship between the aneurysm and its parent vessel may be correlated with aneurysm rupture status (suggesting, by extrapolation, that these factors may also be associated with increased rupture risk for unruptured aneurysms). Chien et al attempt to further our understanding through the use of surface area and volume ratios based on a bounding sphere.

The study of aneurysm morphology remains a challenging endeavor. Integral to the confusion and frustration is the inability to compare prerupture and postrupture characteristics because most individuals with a diagnosed unruptured cerebral aneurysm undergo treatment after discovery and those with a ruptured aneurysm do not have prerupture imaging. To further complicate things, it is debated whether cerebral aneurysms actually change shape with rupture. In addition, it is unclear whether the morphological characteristics seen in increased frequency in ruptured aneurysms are a result of rupture or are higher-risk features associated with rupture. Without a large trial comparing prerupture and postrupture imaging in a cohort of patients deciding to forego treatment, researchers are left to devise new morphological analyses to evaluate the differences in shape seen in unruptured and ruptured aneurysms. Unfortunately, more elaborate imaging and volumetric techniques fail to overcome the same significant limitation. Chien and colleagues report several new parameters that may assist in identifying ruptured aneurysms (ratio of aneurysm volume to bounding sphere > 0.5 and ratio of surface area to bounding sphere < 1.0); however, a definitive understanding of aneurysm morphology will only come after a large, multicenter, collaborative study of prerupture and postrupture imaging is performed in a prospective manner.

**Kyle M. Fargen**  
**J. Mocco**  
 Gainesville, Florida